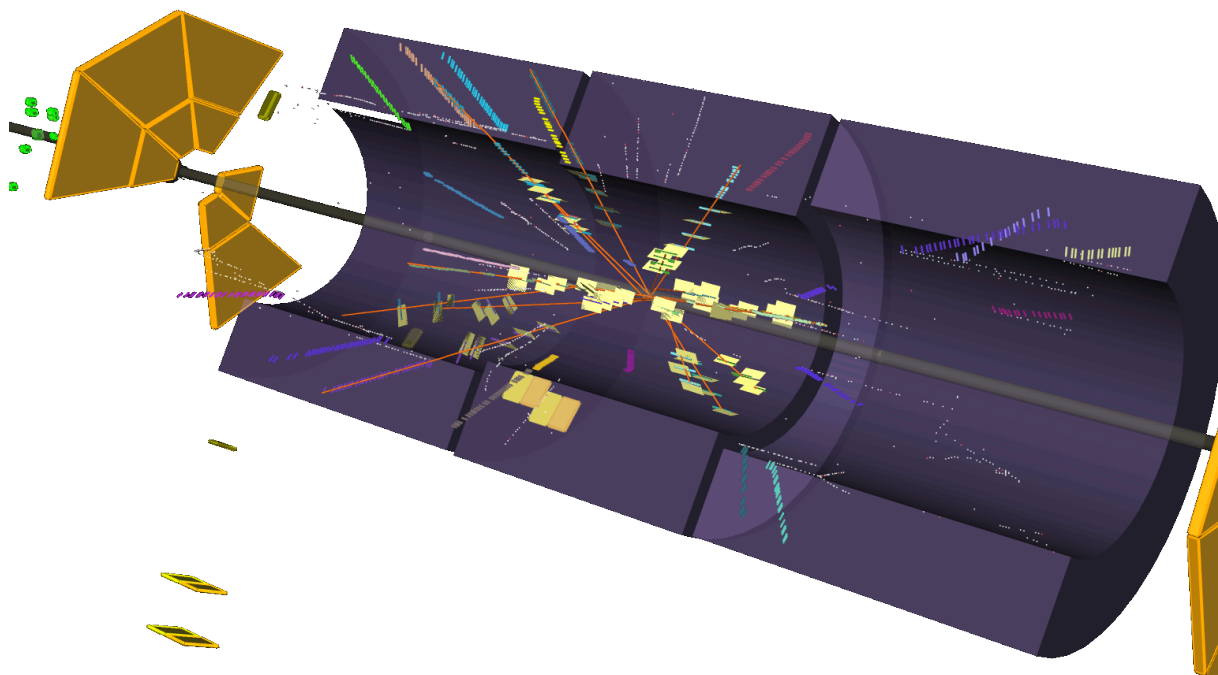


Minimum bias and soft QCD ATLAS Results @ 0.9 and 7 TeV



Roberto Di Nardo

University & INFN Roma Tor Vergata,
On behalf of the ATLAS Collaboration

LC10 Workshop, INFN LNF - 1 December 2010



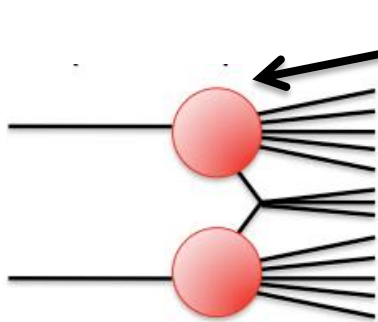
Introduction

- **ATLAS at LHC is a general purpose experiment:**
 - **Main physics goal are: Higgs Boson searches, SUSY, new Heavy Bosons, extradimension...**
- **At the LHC start, in a low luminosity regime, the properties of Minimum Bias events have been investigated, since they are crucial for understanding high- p_T physics.**
- **Moreover, the study of identified particle is important from the **physics** point of view, but also to evaluate the **tracking performance** and calibrate the detector.**
 - **Tuning MC generators**
 - **Compare the production in proton-proton and Heavy Ion collision**
 - **Tracking reconstruction and efficiency, momentum scale**
 - **Secondary vertexing and tracking for long-lived particles**
 - **dE/dx validation**
 - **Alignment**

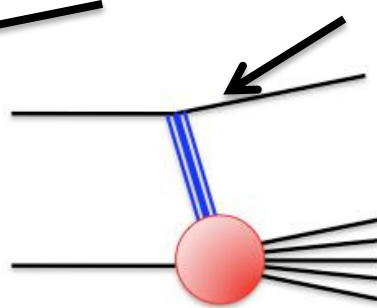


Minimum Bias Events

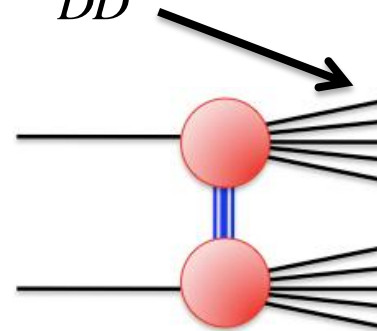
$$\sigma_{tot} = \sigma_{EL} + \sigma_{ND} + \sigma_{SD} + \sigma_{DD}$$



Non-Diffractive (~50 mb)
@7TeV



Single-Diffractive (~14 mb)
@7TeV



Double-Diffractive (~9 mb)
@7TeV

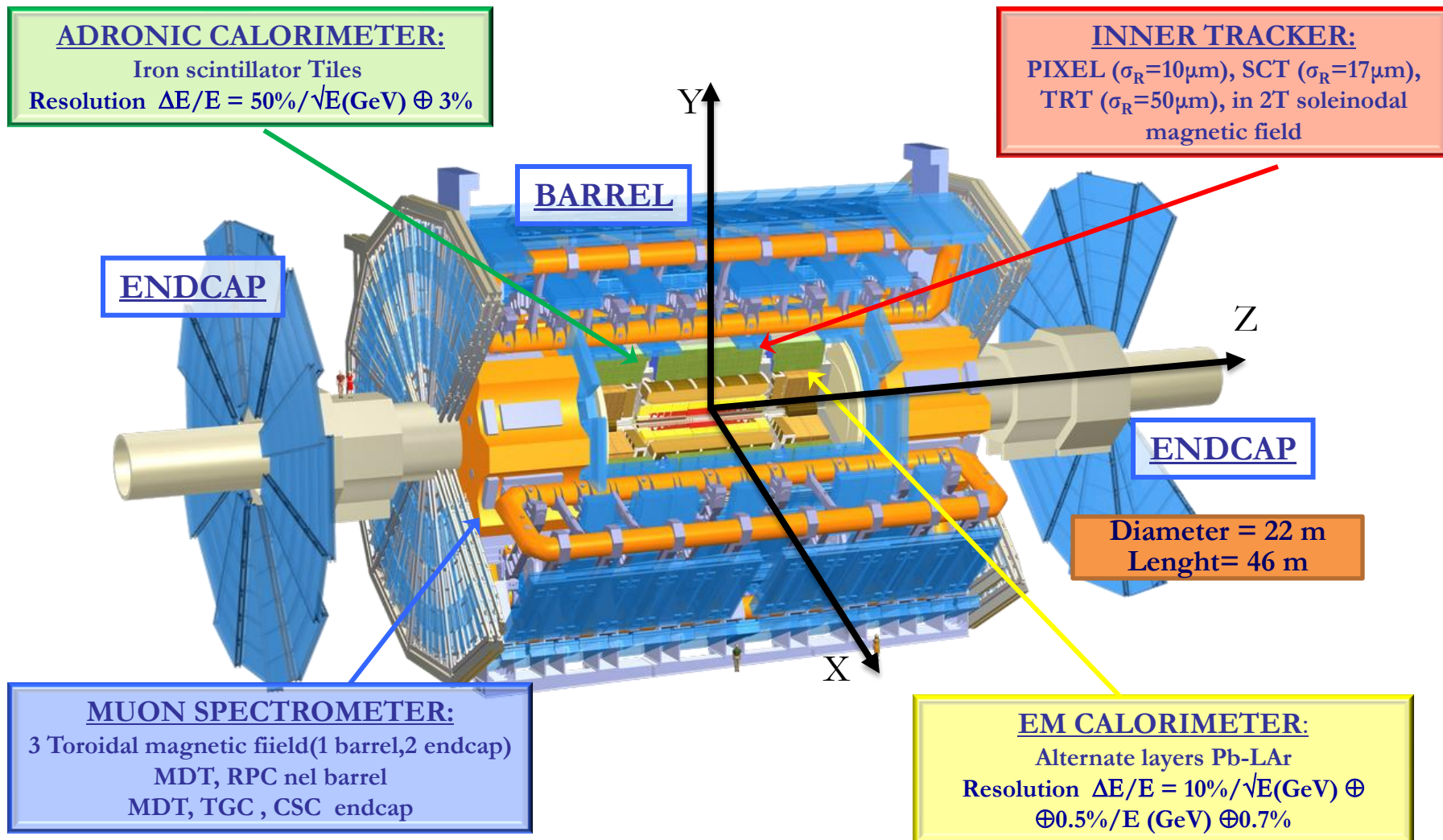
- Soft QCD processes are unavoidable background to all collider observables (in particular jet cross-section, missing energy, isolation cuts...)
- Not well understood since non-perturbative physics is involved.
- Soft QCD distributions have to be used to test the phenomenological models and “tune” the Monte-Carlo event generators to give the best description of the data.
- Visible effect in the tuning also at high- p_T (e.g. colour reconnection)

Outline

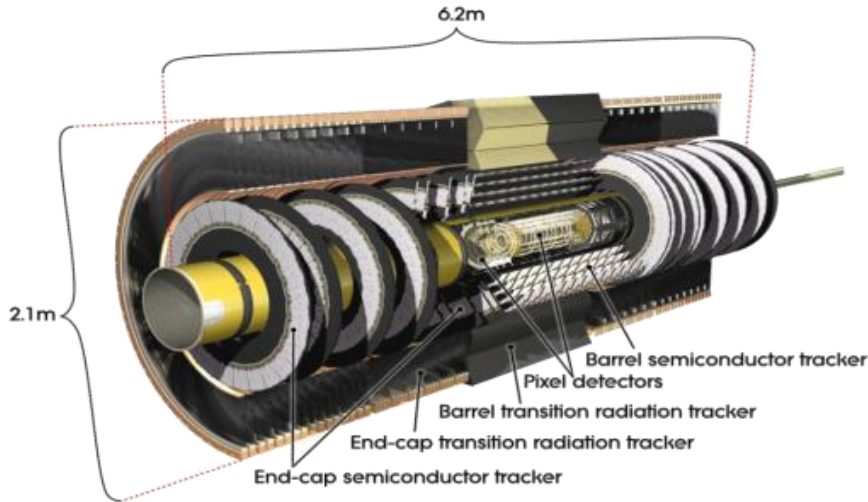
- The ATLAS experiment and the Inner Detector
- Reconstruction of known particles in Minimum Bias Events
- Charged particle multiplicity spectra
- Underlying event measurement
- Angular correlations between charged particles
 - New observable to probe different MB physics models



The ATLAS Experiment



Inner Detector and MB trigger



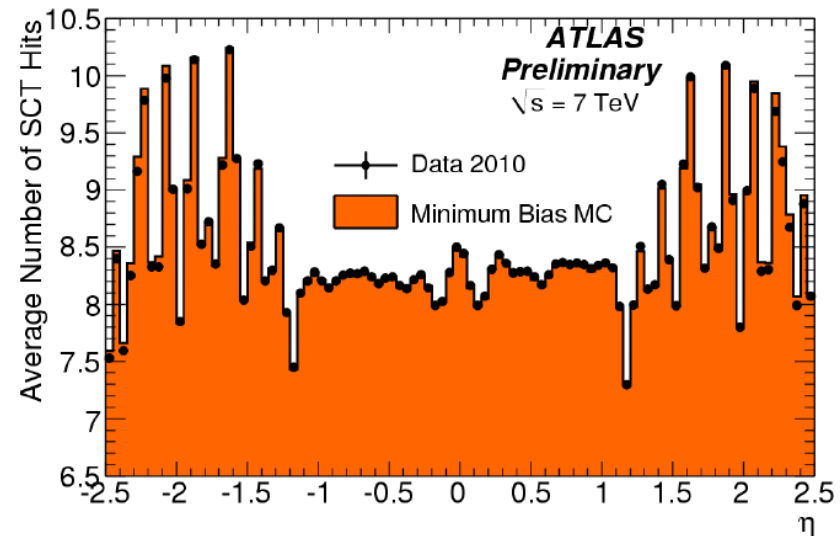
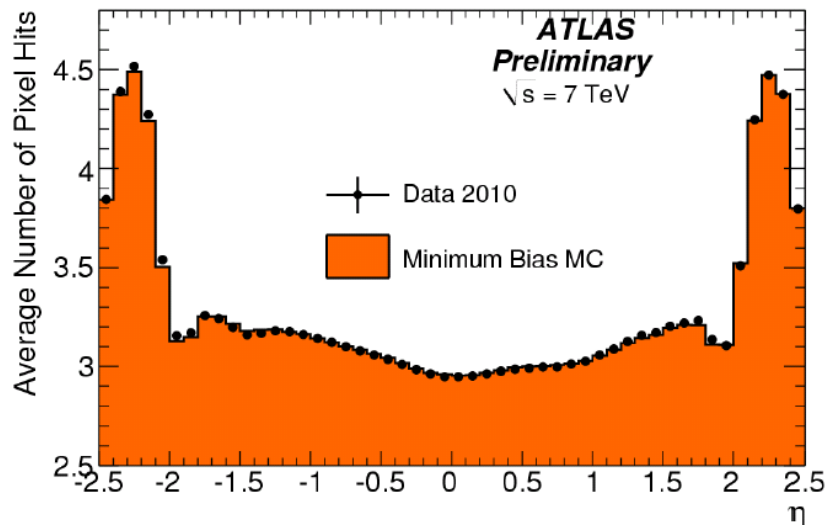
Minimum Bias Trigger Scintillator (MBTS)

- Inside the endcap calorimeters
- 3.6m from interaction point
- Coverage $2.1 < |\eta| < 3.8$ in 2 disks

- Covers $|\eta| < 2.5$ with 3 subdetectors
- **Pixel detector (Silicon Modules)**
 - 1774 modules, ~ 80 M channels
 - Resolutions: $\sim 10 \mu\text{m}$ ($r\phi$) – $\sim 115 \mu\text{m}$ (rz)
- **SCT detector (Silicon Strip)**
 - 4088 modules, ~ 6.3 M channels
 - Resolutions $\sim 17 \mu\text{m}$ ($r\phi$) – $\sim 580 \mu\text{m}$ (rz)
- **TRT detector (straw drift tubes, $|\eta| < 2$)**
 - 176 modules, ~ 0.4 M channels
 - Intrinsic tube resolution $\sim 130 \mu\text{m}$ ($r\phi$)
 - $e^+/-$ PID by detection of transition radiation γ

Detector performances

- Good data/MC agreement in the comparison of the average number of silicon hits on track



- Uncertainty in the detector material description in simulation → largest systematic uncertainties in the measurement
 - 10 % material uncertainty reflects into 3% difference in the efficiency

Known particle reconstruction

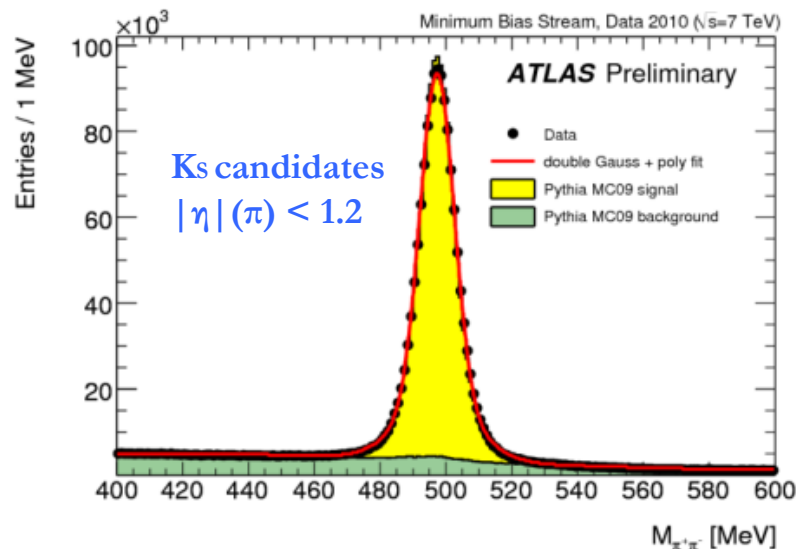


K_s^0 and Λ^0 reconstruction

- $\sim 190 \mu\text{b}^{-1}$ of 7 TeV minimum-bias collision data compared with non-diffractive minimum bias simulation (Pythia ATLAS MC09 tune)
- MC signal and background adjusted separately to match signal/background ratio in data
- Pre-selection: tracks with opposite charge, $p_T > 100 \text{ MeV}$, at least 2 silicon hit (Pixel + SCT)

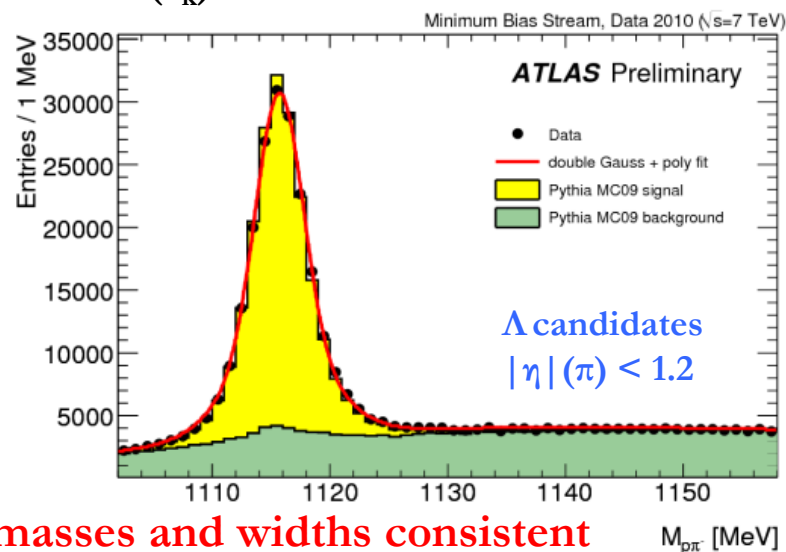
$K_s^0 \rightarrow \pi^+ \pi^-$ ($c\tau = 2.7 \text{ cm}$, $\text{BF} \sim 69\%$)

- Transverse Flight Distance $> 4 \text{ mm}$
- $\text{Cos}(\theta_k) > 0.999$
- Angle between momentum and flight direction



$\Lambda \rightarrow p^+ \pi^- + \text{c.c.}$ ($c\tau = 7.9 \text{ cm}$, $\text{BF} \sim 64\%$)

- Flight Distance $> 30 \text{ mm}$
- $\text{Cos}(\theta_k) > 0.9998$



Fitted masses and widths consistent with MC and PDG mass values



η for K_s^0 , Λ and $\bar{\Lambda}$ candidates

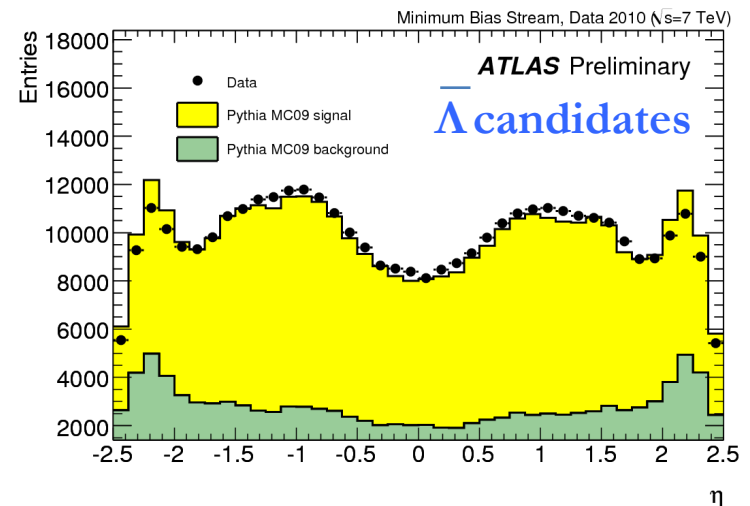
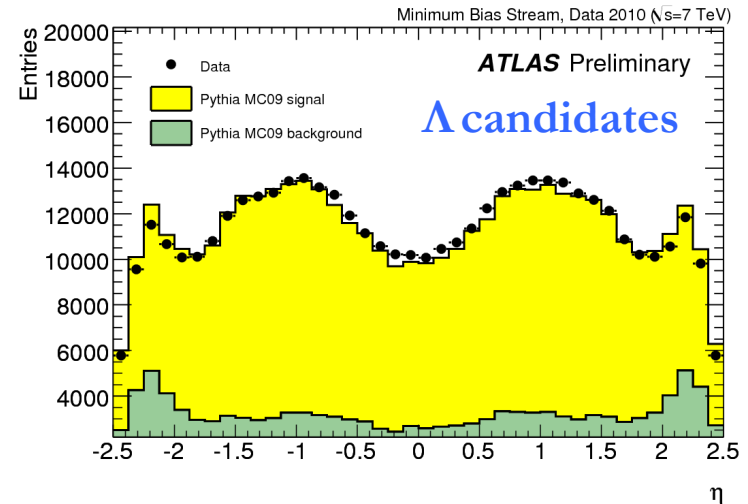
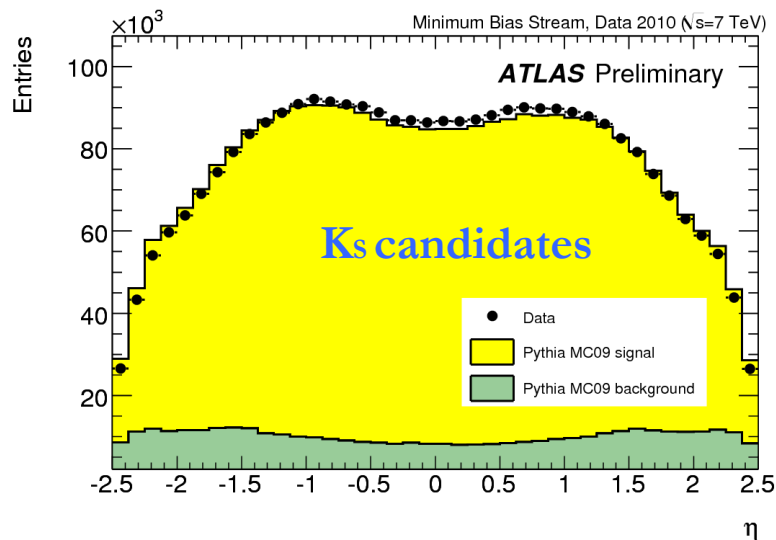
➤ No Correction for detector effect applied

Candidates definitions

➤ $|M(K_s) - M(K_{PDG})| < 20 \text{ MeV}$

➤ $|M(\Lambda) - M(\Lambda_{PDG})| < 7 \text{ MeV}$

➤ MC consistent with data within 10%



Proper decay time for K_s^0 , Λ and $\bar{\Lambda}$

➤ No Correction for detector effect applied

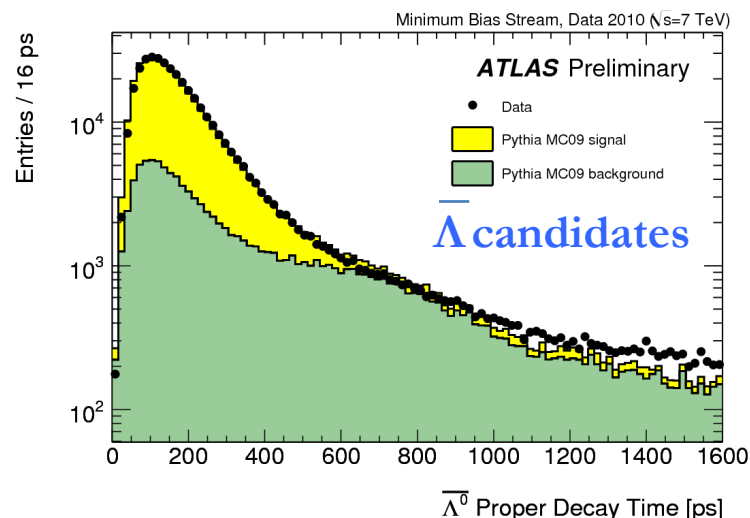
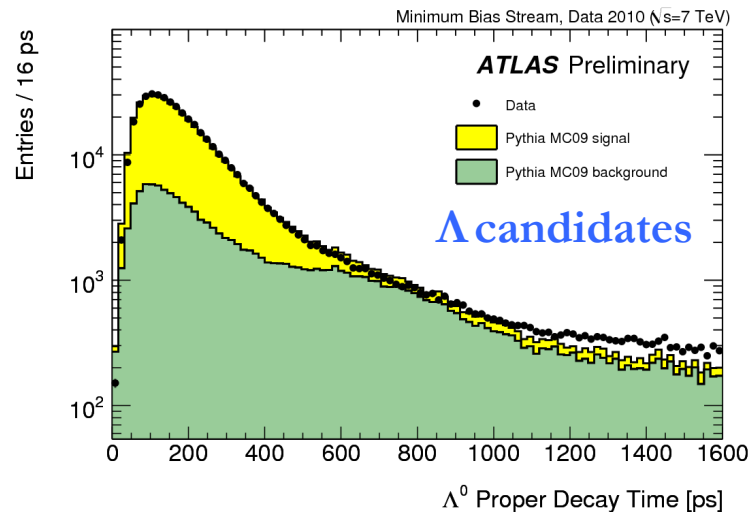
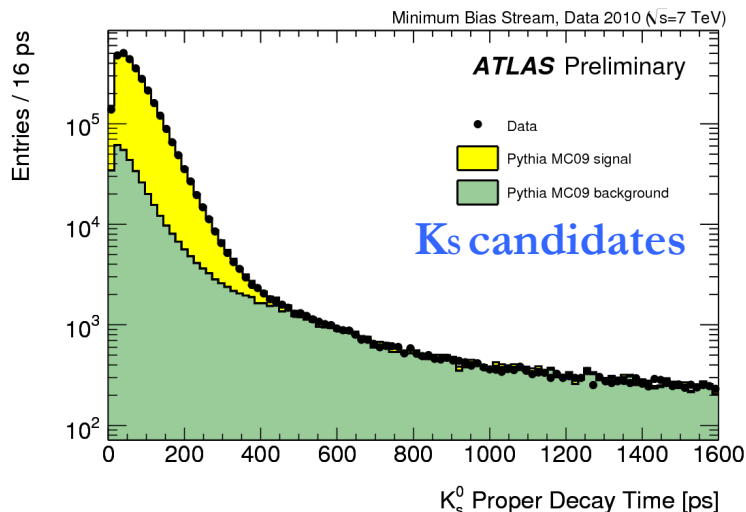
Candidates definitions

➤ $|M(K_s) - M(K_{PDG})| < 20 \text{ MeV}$

➤ $|M(\Lambda) - M(\Lambda_{PDG})| < 7 \text{ MeV}$

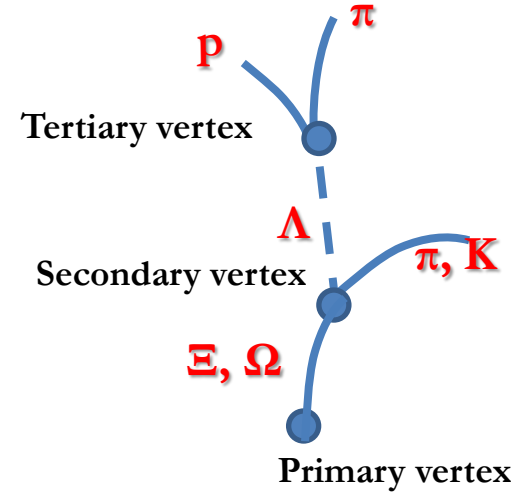
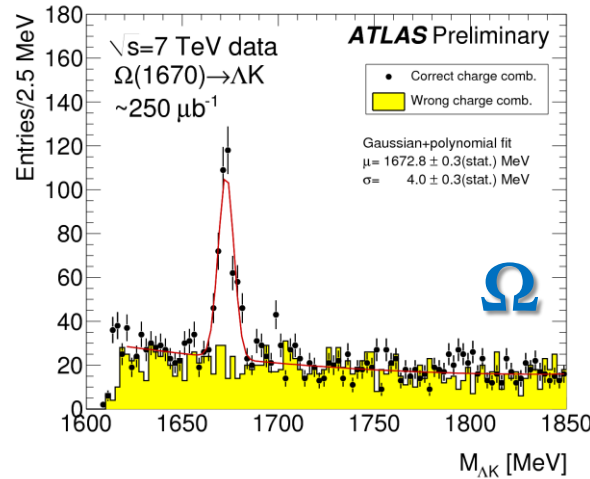
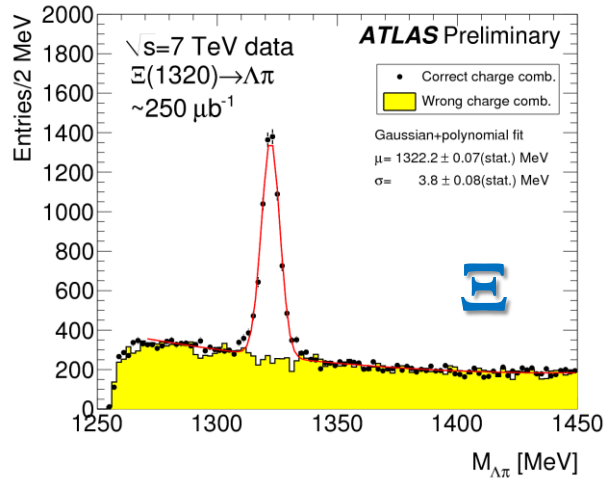
➤ MC in good agreement with data

➤ Works in background dominated region for Λ and $\bar{\Lambda}$

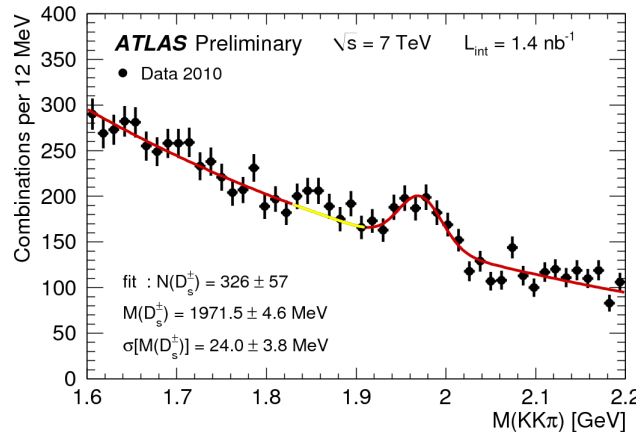
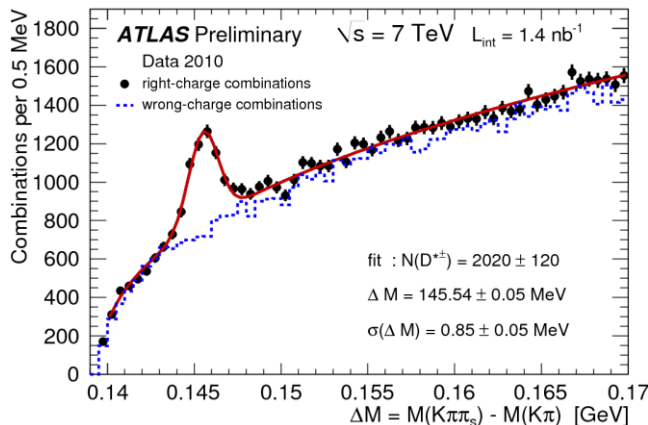


Not only K_s^0 and Λ

$\Xi^- \rightarrow \Lambda \pi^- + \text{c.c.}$ and $\Omega^- \rightarrow \Lambda K^- + \text{c.c.}$



$D^{*+} \rightarrow D^0 (K^- \pi^+) \pi_s^+ + \text{c.c.}$ and $D_s^+ \rightarrow \Phi (K^+ K^-) \pi^+$



Fitted masses and widths consistent with MC and PDG mass values

Charged particle multiplicity spectra

Dataset and Event Selection

The Datasets:

$\sqrt{s}=0.9 \text{ TeV}$
($\sim 7 \mu\text{b}^{-1}$)

$\left\{ \begin{array}{l} 360\text{k events} \\ 4.5\text{M tracks} \end{array} \right.$

$\sqrt{s}=7 \text{ TeV}$
($\sim 190 \mu\text{b}^{-1}$)

$\left\{ \begin{array}{l} 10\text{M events} \\ 210\text{M tracks} \end{array} \right.$

The Event Selection:

- MBTS single-cell trigger in coincidence with the BPTX (beam pickup)
- 1 Vertex reconstructed
 - 2 tracks + Beam Spot
 - No pileup (secondary vtx with >3 tracks)

Most inclusive

- ≥ 2 good tracks
- $p_T > 100 \text{ MeV} ; |\eta| \leq 2.5$
- Additional tracking algorithm at low p_T

Negligible diffractive contribution

- ≥ 6 good tracks
- $p_T > 500 \text{ MeV} ; |\eta| \leq 2.5$
- Additional tracking algorithm at low p_T



Correction procedure

- Event-wise correction for trigger and vertex efficiencies

$$w_{ev}(n_{sel}^{BS}) = \frac{1}{\mathcal{E}_{trig}(n_{sel}^{BS})} \cdot \frac{1}{\mathcal{E}_{vertex}(n_{sel}^{BS})}$$

n_{sel}^{BS} : number of tracks; cuts as close to final selection as possible without a vertex

- Track-wise correction (e.g. tracking efficiency)

$$w_{ev}(p_T, \eta) = \frac{1}{\mathcal{E}_{trk}(p_T, \eta)} \cdot (1 - f_{sec}(p_T, \eta)) \cdot (1 - f_{okr}(p_T, \eta))$$

Fraction of tracks out of kinematic range

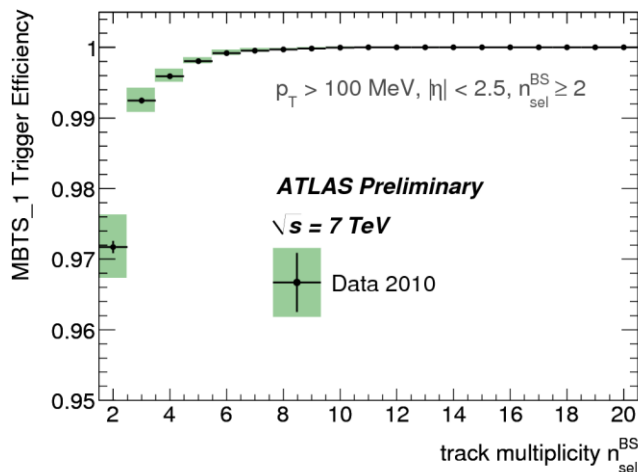
Fraction of secondaries

- Takes in to account secondary contamination and tracks out of kinematic range
 - e.g. Track $p_T < 100$ MeV but particle $p_T > 100$ MeV
- N_{ch} and p_T both corrected using a Bayesian unfolding
- $\langle p_T \rangle$ vs $n_{ch} \rightarrow$ bin-by-bin correction of average p_T and the n_{ch} migration

Efficiencies

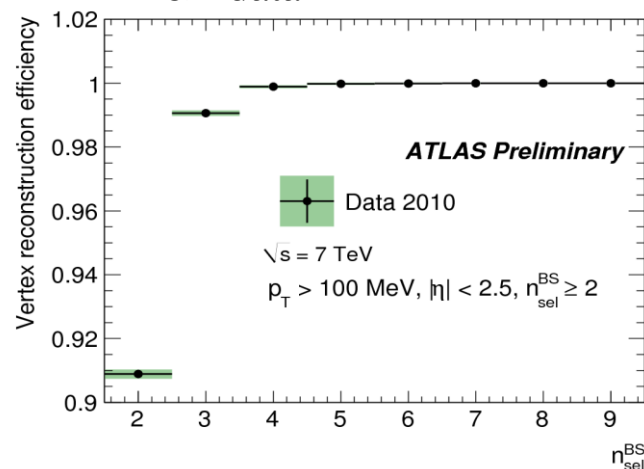
ϵ_{trig}

Trigger efficiency from data using orthogonal trigger



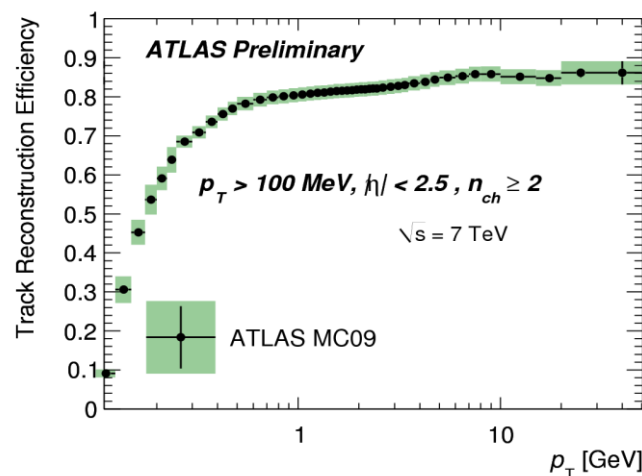
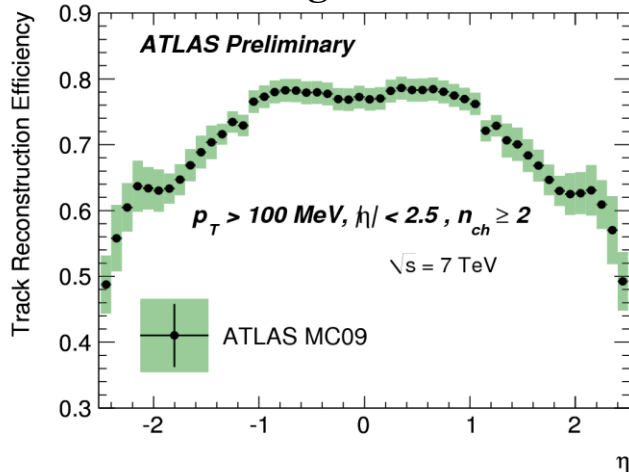
ϵ_{vtx}

Vertex efficiency measured from data



ϵ_{trk}

Tracking efficiency from MC – systematic dominated by knowledge of material budget



$$1/N_{ev} dN_{ch}/d\eta$$

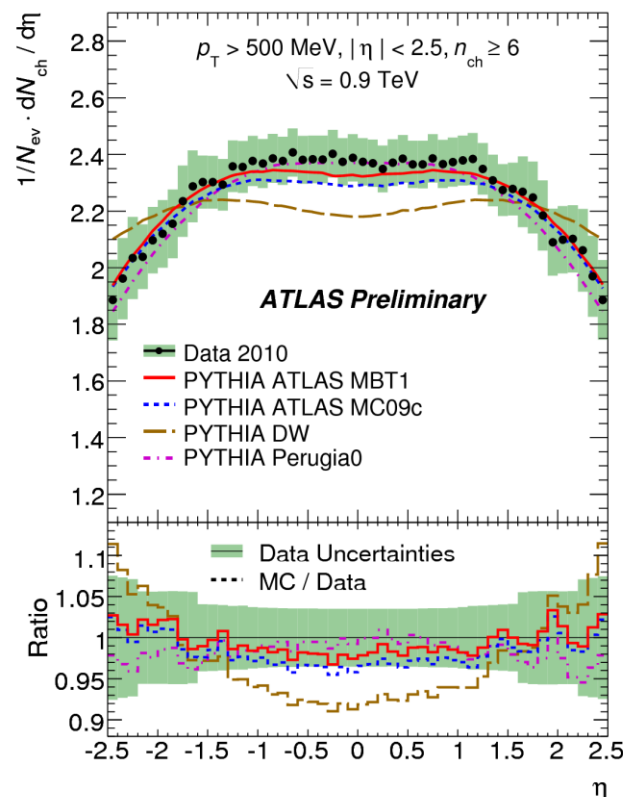
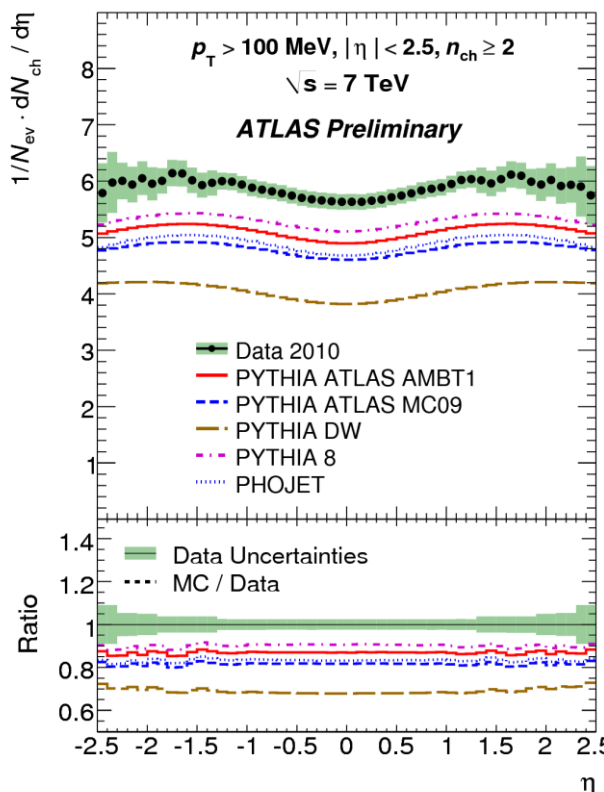
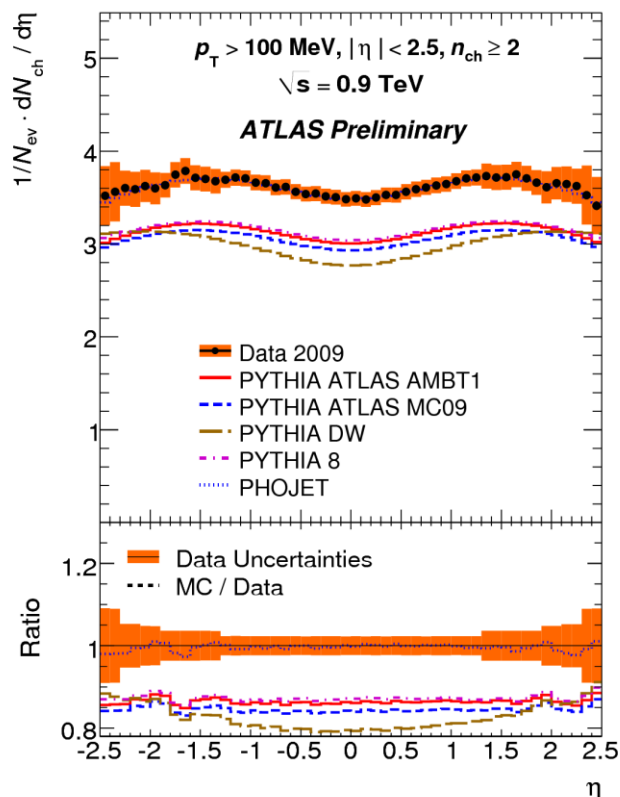
➤ Different models differ in normalization but the shape are almost similar

➤ Track multiplicity underestimated.

➤ Very little shape variation between models

➤ $n_{ch} \geq 6$, $p_T > 500 \text{ MeV}$ measurement used in AMBT1 tune

gata



$n_{ch} \geq 2, p_T > 100 \text{ MeV}$

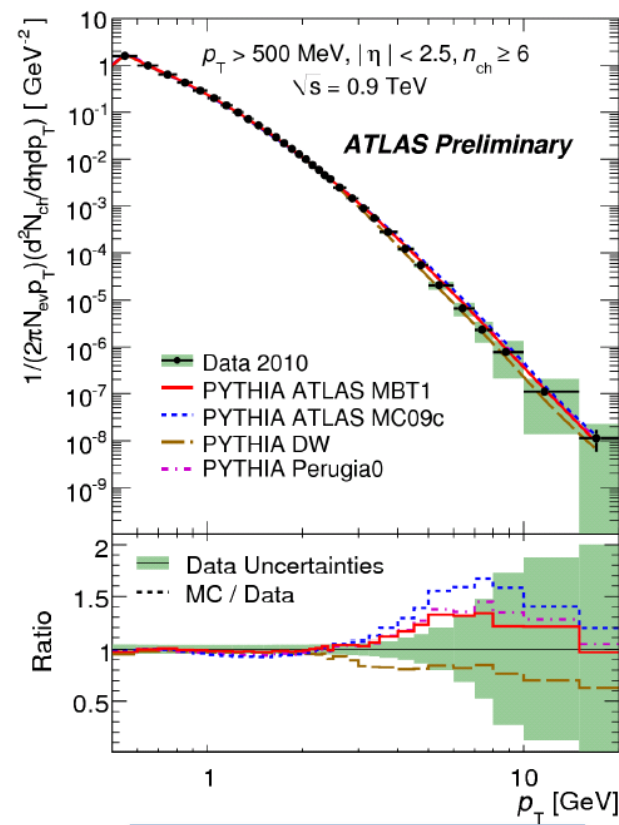
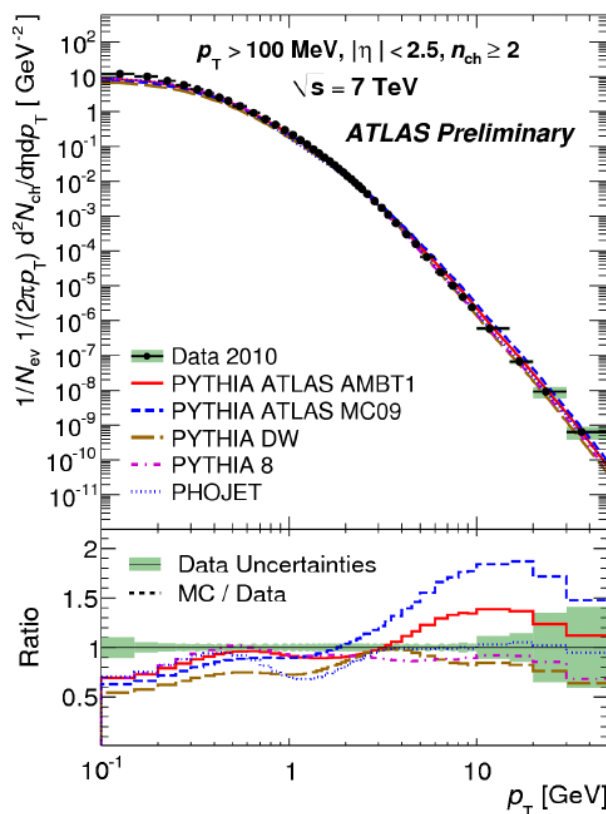
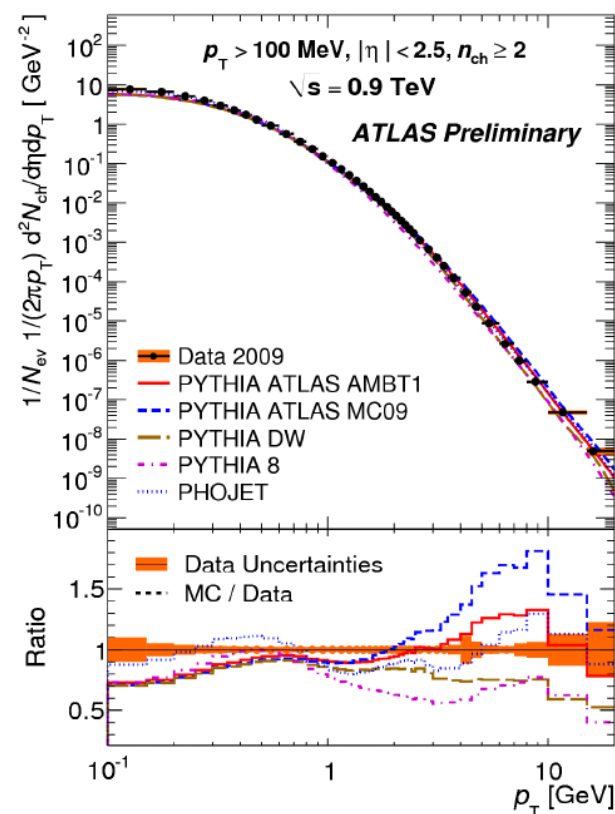
$n_{ch} \geq 6, p_T > 500 \text{ MeV}$



$$1/(2\pi p_T) 1/N_{ev} d^2N_{ch}/d\eta dp_T$$

- Measurement spans 10 orders of magnitude
- Large disagreement at low p_T and high p_T
- Improvement at medium p_T for AMBT1 tune

rgata



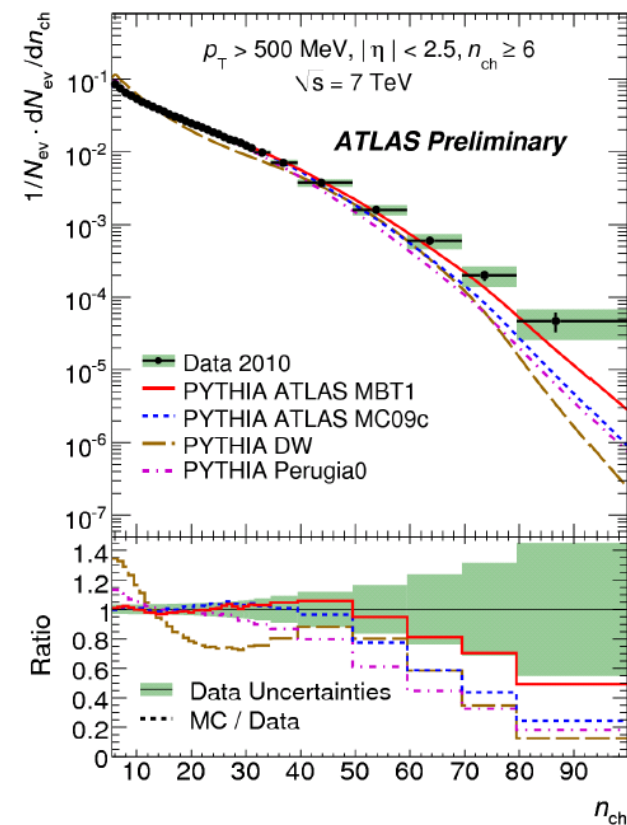
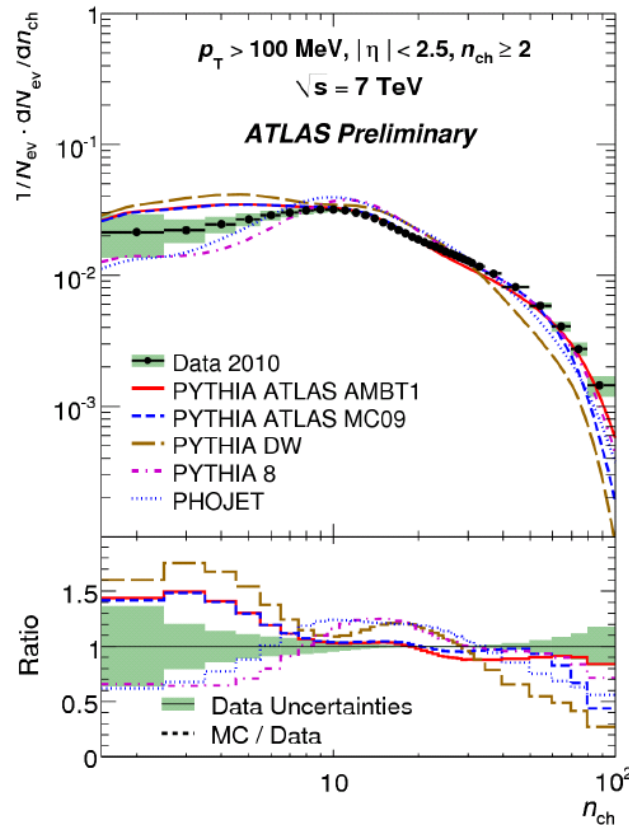
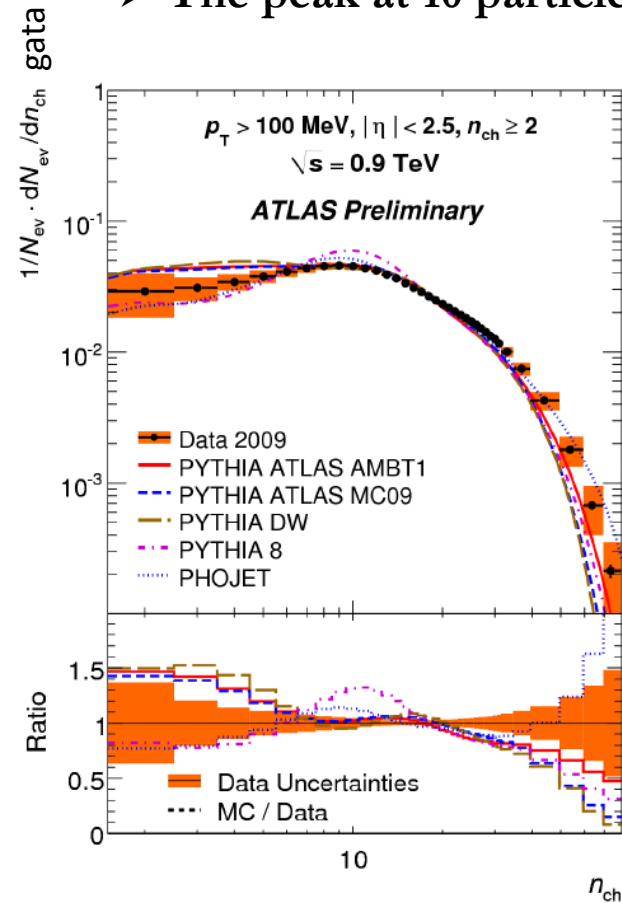
$n_{ch} \geq 2, p_T > 100 \text{ MeV}$

$N_{ch} \geq 6, p_T > 500 \text{ MeV}$



$$1/N_{\text{ev}} dN_{\text{ev}}/dN_{\text{ch}}$$

- The low n_{ch} region not well modeled by any MC
 - large contribution from diffraction
- The peak at 10 particles well described by AMBT1



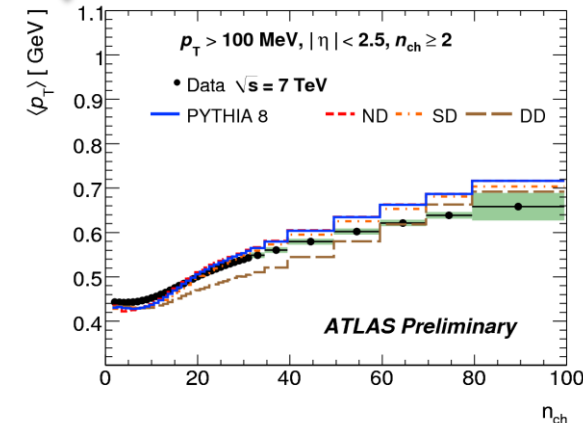
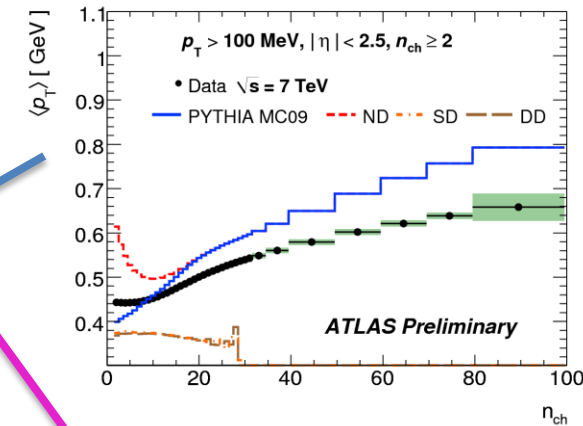
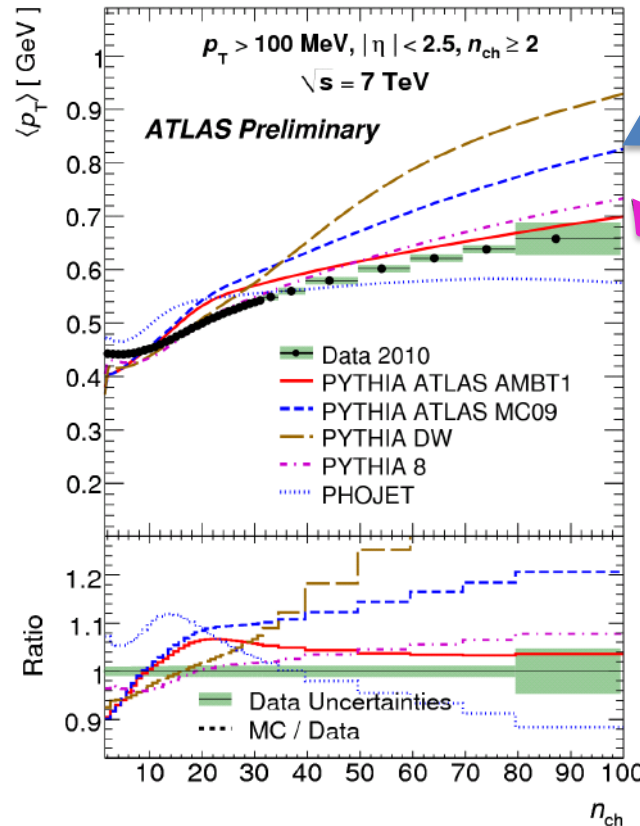
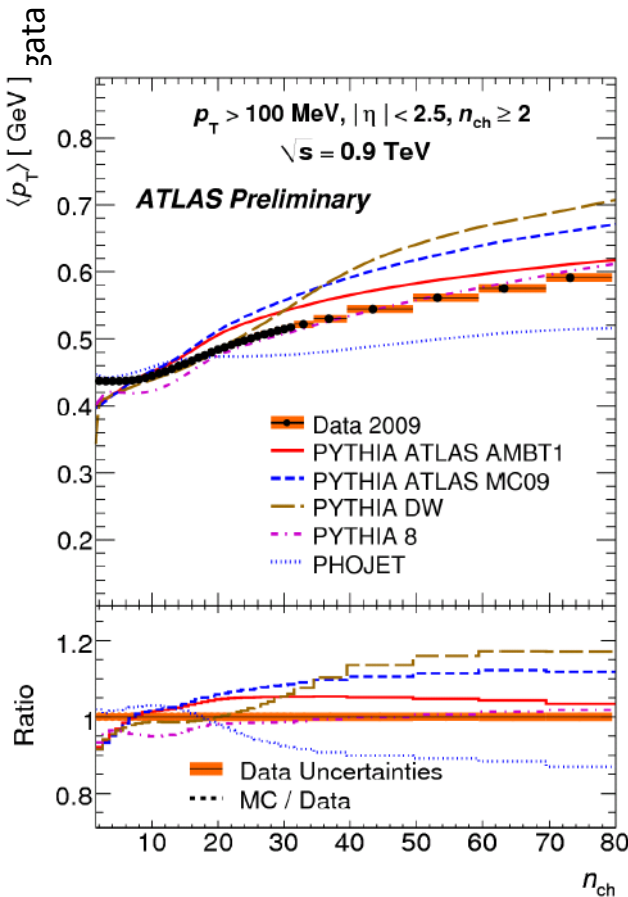
$n_{\text{ch}} \geq 2, p_T > 100 \text{ MeV}$

$N_{\text{ch}} \geq 6, p_T > 500 \text{ MeV}$



$\langle p_T \rangle$ vs N_{ch}

- Best description from AMBT1 and Pythia8
- Shape at high p_T well modelled
- High sensitivity of the low n_{ch} shape linked to the different ND,SD,DD fractions



Pythia6 – softer spectrum at low n_{ch} – too large diffractive component?

$n_{ch} \geq 2, p_T > 100 \text{ MeV}$

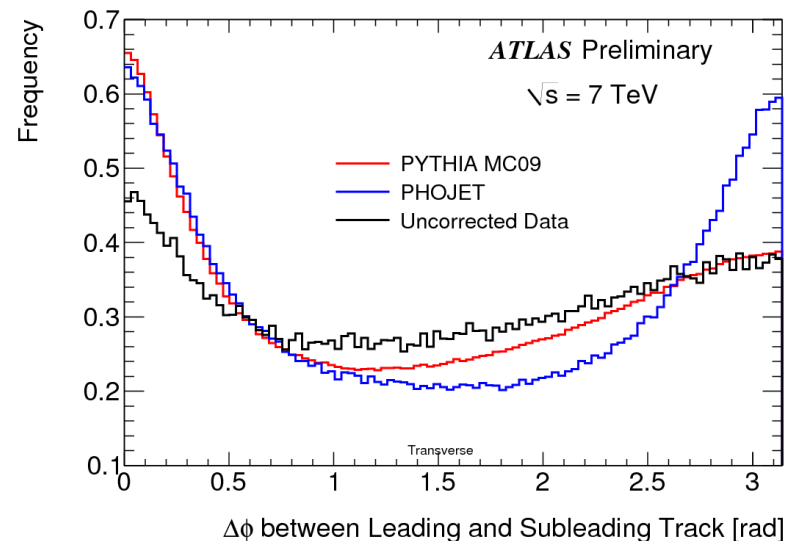
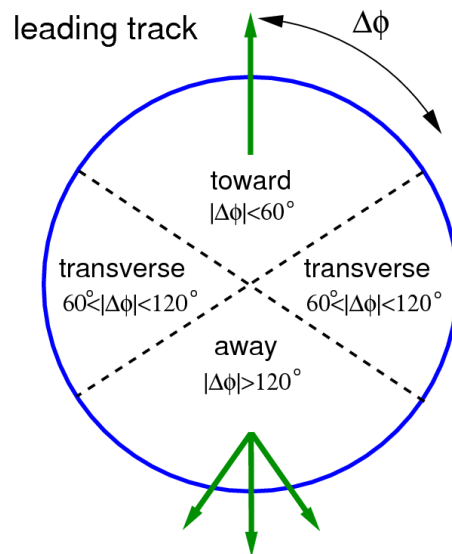


Underlying event



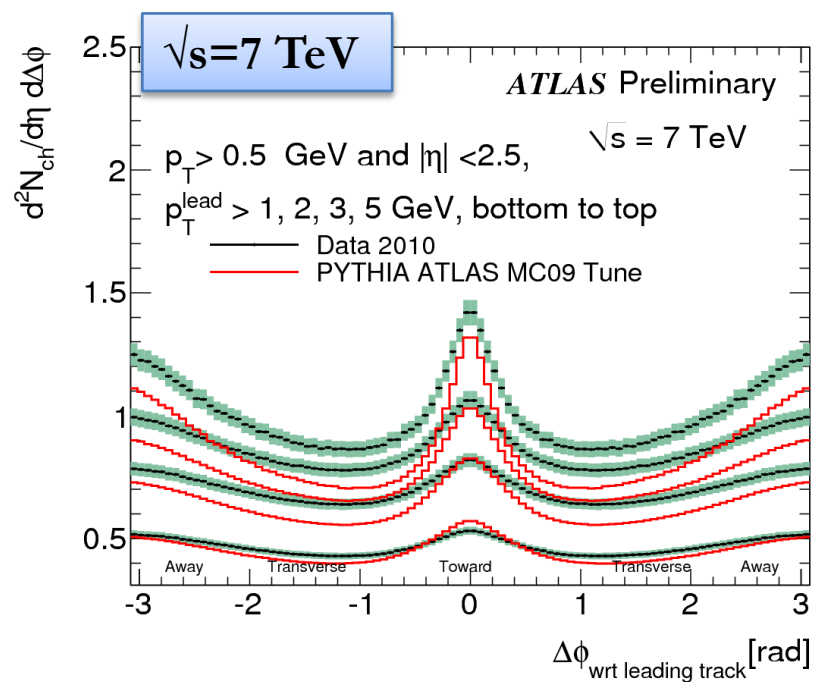
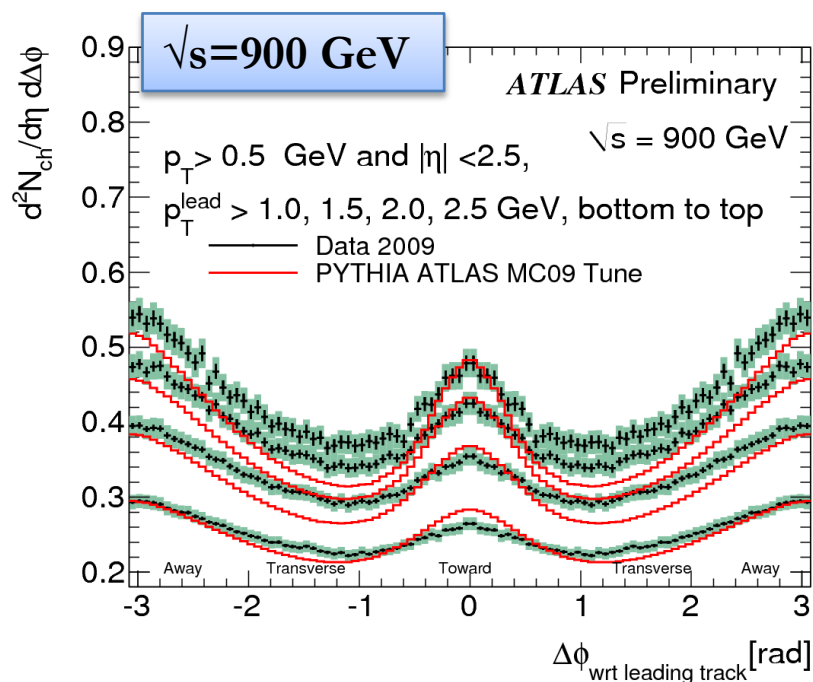
Underlying event

- “Underlying Event”: everything else in addition the hard scattering process
 - MPI, ISR-FSR contributions, beam-beam remnants
- The sensitive region to the UE is the one perpendicular to the hard scattering (transverse region) – Used the leading track to identify the leading jet
 - $60^\circ < |\Delta\phi| < 120^\circ$
- same correction for trigger, vertex and tracking efficiency as in the Minimum Bias



Angular distributions vs p_T^{lead}

- Charged particle number density for tracks other than the leading track
 - plot reflected wrt $\Delta\phi=0$
 - Jet-like shape (higher tracks population in the toward and the away region) is much evident for harder leading tracks

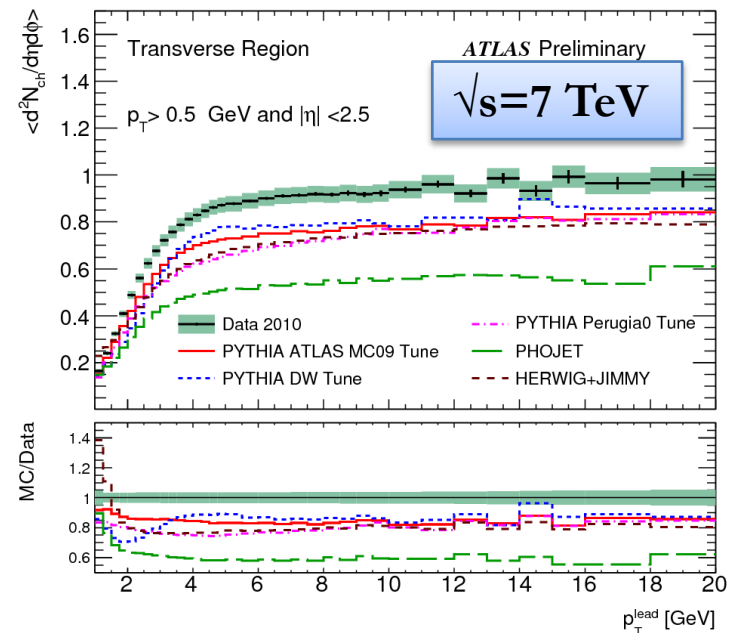
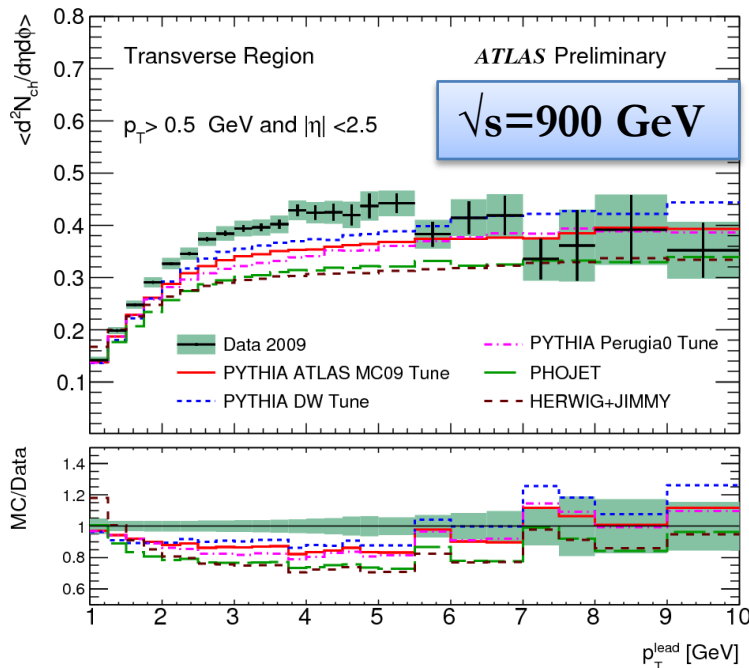


- different densities and different angular distributions between data and MC



Multiplicity

➤ Density of charged particle ($p_T > 500 \text{ MeV}$ $|\eta| < 2.5$) as function of the leading track p_T in the transverse region increase of a factor 2 from 900 GeV to 7 TeV.



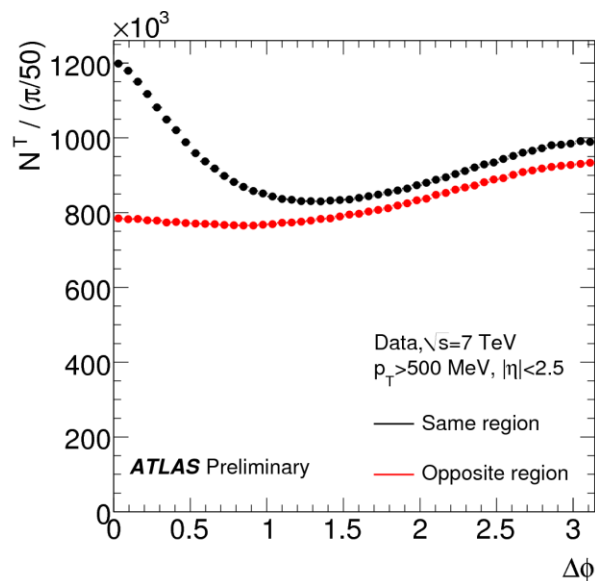
➤ Plateau value is a factor 2 larger as seen in the Minimum Bias events (due to the high p_T track selection effect: more momentum exchange and lack of diffractive contributions in events with p_T^{lead} in plateau region)



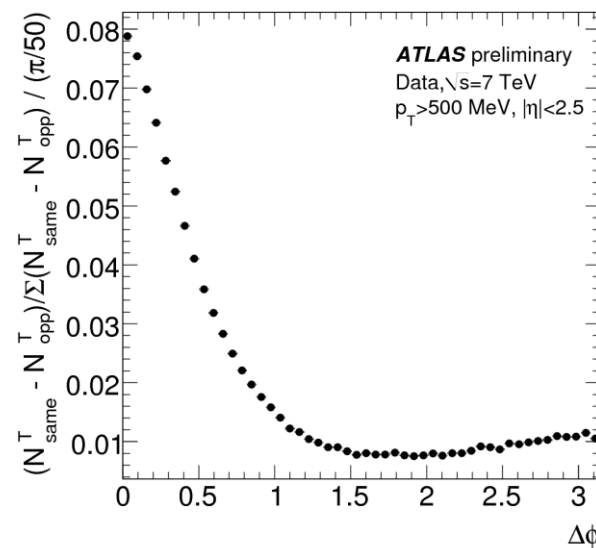
Angular Correlations

Angular correlations

- $\Delta\Phi$ = difference of the azimuthal angle between the p_T -leading track and all the other non leading tracks in the event
- Studied the “Toward” and “Away” components (width and weight of the “Toward” and “Away” peaks) – variable sensible to differences between models
 - This variable has been measured in the **same** and in the **opposite** regions with respect to the leading one (in η)



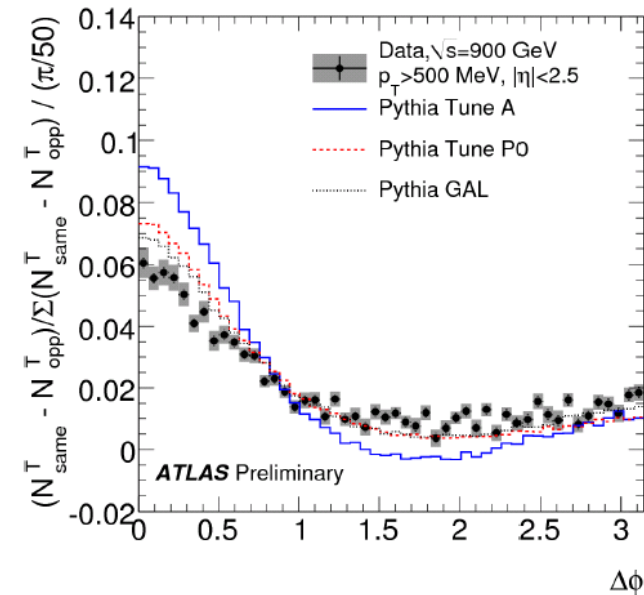
More particles produced in the same region



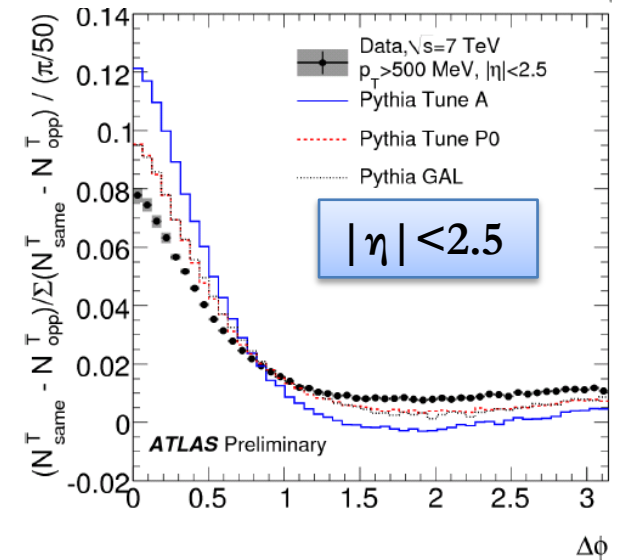
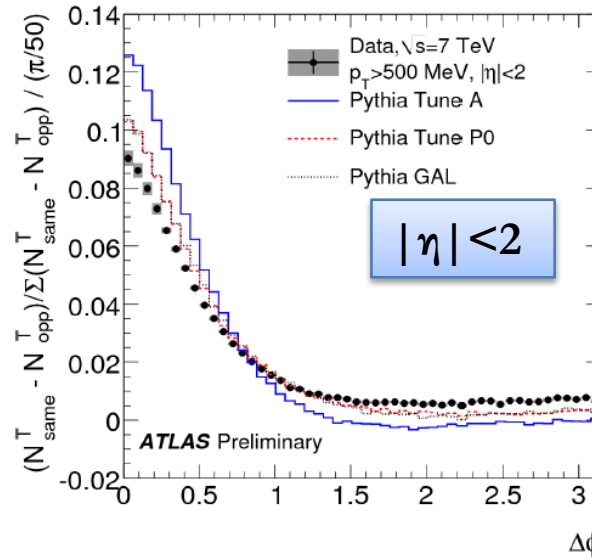
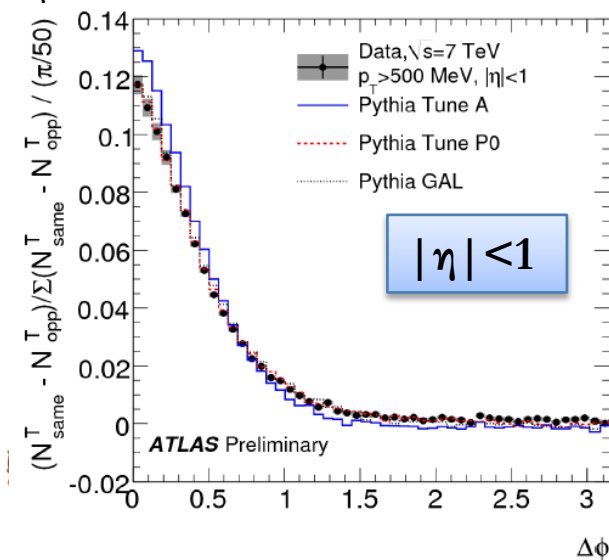
“same minus opposite” $\Delta\Phi$ normalized

The $\Delta\varphi$ crest shape

- Good consistency in central pseudorapidity region $|\eta| < 1$
- Considering also the forward regions comes out that models poorly constrained at forward direction where reach of previous experiments limited
- Same discrepancy observed @ 0.9 TeV



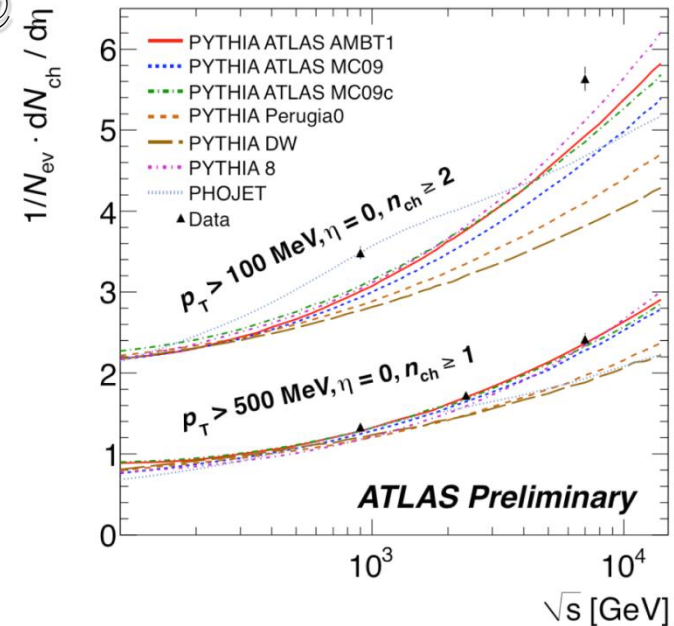
University & INFN Tor Vergata



Conclusions

➤ Spectra of charged particle measured from 100 MeV @ 0.9, 2.36 and 7 TeV

- no model dependent correction applied (well-defined phase-space and no correction back to a particular component (e.g. NSD))
- $p_T > 100$ MeV
 - Models underestimate the particle multiplicity
- $p_T > 500$ MeV
 - Good description of the data by AMBT1



- Track based underlying event measurements have been performed by ATLAS
 - None of the current models can describe accurately all the UE measurement
 - Can be used as input to improve the models
- Angular correlations: new observable sensible to different models
 - Can be used to improve the tunings



References

Reconstruction of known particle @ 7 TeV

K_s^0 and Λ^0 reconstruction

ATLAS-CONF-2010-033

Ξ , Ω , $K^*(890)$

ATLAS-CONF-2010-032

D^* mesons reconstruction

ATLAS-CONF-2010-034

Inclusive charged particle spectra @ 0.9 and 7 TeV

$p_T > 100$ MeV, $N_{ch} > 1$, $|\eta| < 2.5$

ATLAS-CONF-2010-046

$p_T > 500$ MeV, $N_{ch} > 9$, $|\eta| < 2.5$

Phys. Lett. B 688, 1, ATLAS-CONF-2010-024

$p_T > 500$ MeV, $N_{ch} > 6$, $|\eta| < 2.5$

ATLAS-CONF-2010-047 (2.36 TeV)

(diffraction suppressed sample, used to derive AMBT1)

ATLAS-CONF-2010-031

Underlying event using tracks

Angular correlation between charged particles

ATLAS-CONF-2010-081

-Measurements probing event topologies @ 0.9 and 7 TeV ($p_T > 500$ MeV)

ATLAS-CONF-2010-082





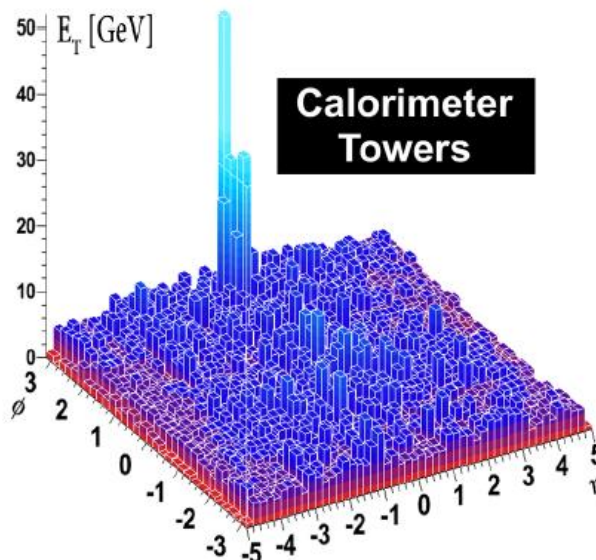
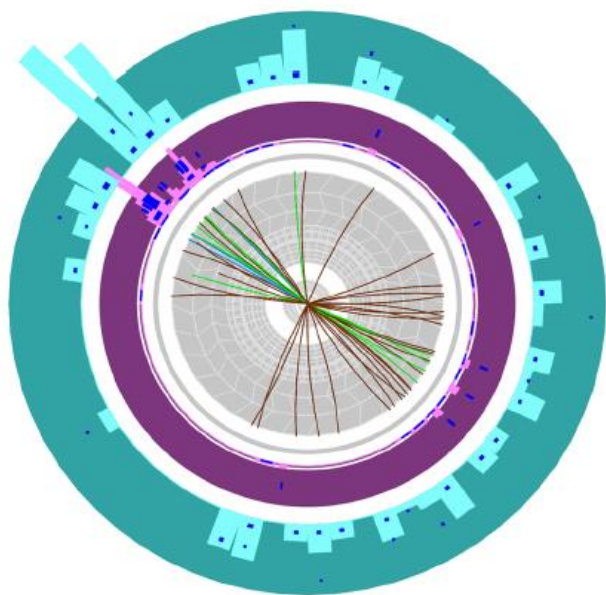
Extra

ATLAS HI hot results

- The LHC heavy ion program – Pb-Pb collisions → opportunity to study jet quenching at much higher jet energies than achieved at RHIC.
- Data taken since the beginning of November, $\sqrt{s_{NN}} = 2.76$ TeV – $1.7 \mu\text{b}^{-1}$ of data used
- At this energy, NLO calculation predict high rate of jets above 100 GeV in $|\eta| < 4.5$
- Focus on the balance between pair of jets with highest E_T and $\Delta\phi$ separation $|\phi_1 - \phi_2| > \pi/2$
- Jet Energy unbalance studied in terms of asymmetry

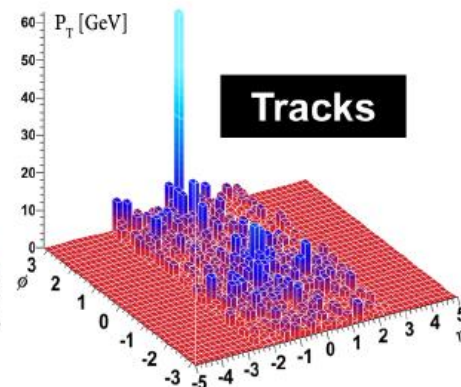
$$A_J = \frac{E_{T1} - E_{T2}}{E_{T1} + E_{T2}}, \Delta\phi > \frac{\pi}{2}$$

$$E_{T1} > 100 \text{ GeV}, E_{T2} > 25 \text{ GeV}$$



ATLAS

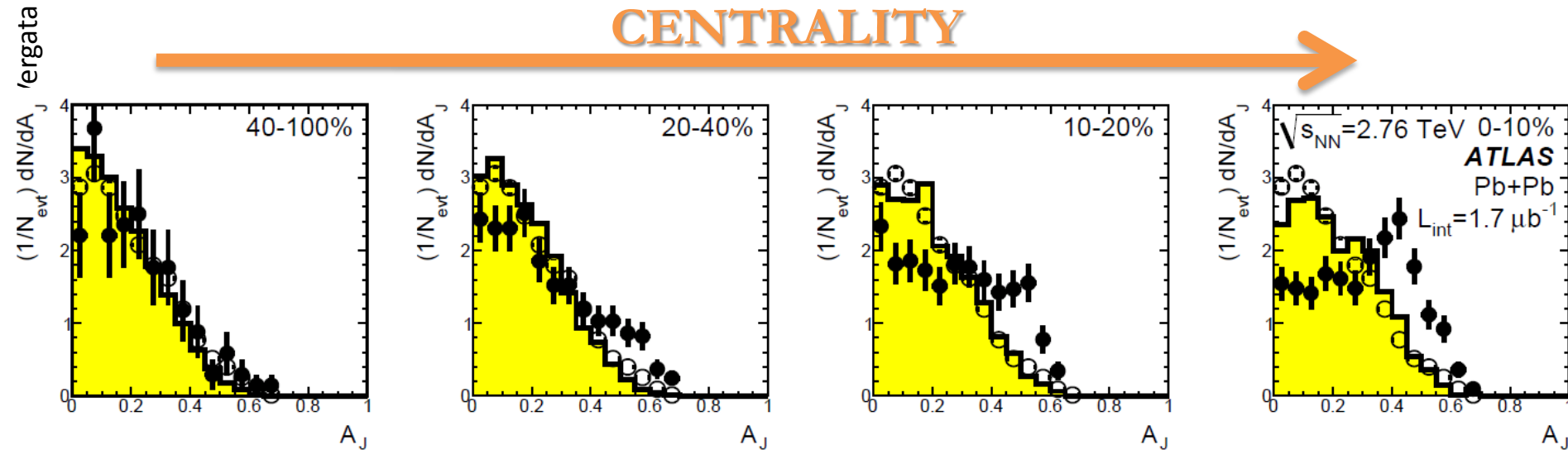
Run: 169045
Event: 1914004
Date: 2010-11-12
Time: 04:11:44 CET



ATLAS HI hot results

- Dijet events are expected to have A_J near zero
 - Deviations from gluon radiation falling outside the jet cone and instrumental effects.

CENTRALITY



Histogram: MC (PYTHIA+HIJING) | open points: 7 TeV pp data | filled: Pb-Pb data

- **Dijet asymmetry observed in PbPb data and not in p-p collisions**
- **May point to an interpretation in terms of strong jet energy loss in a hot, dense medium**

Backup



Tunings

- The basic components of Pythia that require tuning are the descriptions of:
 - Final state radiation and hadronisation,
 - Initial state radiation and primordial k_T ,
 - Underlying event, beam remnants, colour reconnection, and
 - Energy scaling.

- Perugia0
 - PYTHIA Tune based on Minimum bias results from CDF and UA5. No UE data used
 - CTEQ5L parton distribution functions used
- DW
 - PYTHIA Tune that use CDF UE and Drell-Yan data (no Min Bias Data)
- ATLAS MC09
 - PYTHIA Tune based on CDF Minimum Bias and UE Measurements (RUN I and II) plus the D0 results on dijet angular correlations



ATLAS data in AMBT1

Analysis	Observable	Tuning range
ATLAS 0.9 TeV, minimum bias, $n_{\text{ch}} \geq 6$	$\frac{1}{N_{\text{ev}}} \cdot \frac{dN_{\text{ch}}}{d\eta}$	-2.5 – 2.5
ATLAS 0.9 TeV, minimum bias, $n_{\text{ch}} \geq 6$	$\frac{1}{N_{\text{ev}}} \cdot \frac{1}{2\pi p_T} \cdot \frac{d^2 N_{\text{ch}}}{d\eta dp_T}$	≥ 5.0
ATLAS 0.9 TeV, minimum bias, $n_{\text{ch}} \geq 6$	$\frac{1}{N_{\text{ev}}} \cdot \frac{dN_{\text{ev}}}{dn_{\text{ch}}}$	≥ 20
ATLAS 0.9 TeV, minimum bias, $n_{\text{ch}} \geq 6$	$\langle p_T \rangle$ v.s. n_{ch}	≥ 10
ATLAS 0.9 TeV, UE in minimum bias	$\langle \frac{d^2 N_{\text{chg}}}{d\eta d\phi} \rangle$ (towards)	≥ 5.5 GeV
ATLAS 0.9 TeV, UE in minimum bias	$\langle \frac{d^2 N_{\text{chg}}}{d\eta d\phi} \rangle$ (transverse)	≥ 5.5 GeV
ATLAS 0.9 TeV, UE in minimum bias	$\langle \frac{d^2 N_{\text{chg}}}{d\eta d\phi} \rangle$ (away)	≥ 5.5 GeV
ATLAS 0.9 TeV, UE in minimum bias	$\langle \frac{d^2 \sum p_T}{d\eta d\phi} \rangle$ (towards)	≥ 5.5 GeV
ATLAS 0.9 TeV, UE in minimum bias	$\langle \frac{d^2 \sum p_T}{d\eta d\phi} \rangle$ (transverse)	≥ 5.5 GeV
ATLAS 0.9 TeV, UE in minimum bias	$\langle \frac{d^2 \sum p_T}{d\eta d\phi} \rangle$ (away)	≥ 5.5 GeV
ATLAS 7 TeV, minimum bias, $n_{\text{ch}} \geq 6$	$\frac{1}{N_{\text{ev}}} \cdot \frac{dN_{\text{ch}}}{d\eta}$	-2.5 – 2.5
ATLAS 7 TeV, minimum bias, $n_{\text{ch}} \geq 6$	$\frac{1}{N_{\text{ev}}} \cdot \frac{1}{2\pi p_T} \cdot \frac{d^2 N_{\text{ch}}}{d\eta dp_T}$	≥ 5.0
ATLAS 7 TeV, minimum bias, $n_{\text{ch}} \geq 6$	$\frac{1}{N_{\text{ev}}} \cdot \frac{dN_{\text{ev}}}{dn_{\text{ch}}}$	≥ 40
ATLAS 7 TeV, minimum bias, $n_{\text{ch}} \geq 6$	$\langle p_T \rangle$ v.s. n_{ch}	≥ 10
ATLAS 7 TeV, UE in minimum bias	$\langle \frac{d^2 N_{\text{chg}}}{d\eta d\phi} \rangle$ (towards)	≥ 10 GeV
ATLAS 7 TeV, UE in minimum bias	$\langle \frac{d^2 N_{\text{chg}}}{d\eta d\phi} \rangle$ (transverse)	≥ 10 GeV
ATLAS 7 TeV, UE in minimum bias	$\langle \frac{d^2 N_{\text{chg}}}{d\eta d\phi} \rangle$ (away)	≥ 10 GeV
ATLAS 7 TeV, UE in minimum bias	$\langle \frac{d^2 \sum p_T}{d\eta d\phi} \rangle$ (towards)	≥ 10 GeV
ATLAS 7 TeV, UE in minimum bias	$\langle \frac{d^2 \sum p_T}{d\eta d\phi} \rangle$ (transverse)	≥ 10 GeV
ATLAS 7 TeV, UE in minimum bias	$\langle \frac{d^2 \sum p_T}{d\eta d\phi} \rangle$ (away)	≥ 10 GeV



Tevatron data in AMBT1

CDF Run I underlying event in dijet events[13] (leading jet analysis)

N_{ch} density vs leading jet p_T (transverse), JET20

N_{ch} density vs leading jet p_T (toward), JET20

N_{ch} density vs leading jet p_T (away), JET20

Σp_T density vs leading jet p_T (transverse), JET20

Σp_T density vs leading jet p_T (toward), JET20

Σp_T density vs leading jet p_T (away), JET20

N_{ch} density vs leading jet p_T (transverse), min bias

N_{ch} density vs leading jet p_T (toward), min bias

N_{ch} density vs leading jet p_T (away), min bias

Σp_T density vs leading jet p_T (transverse), min bias

Σp_T density vs leading jet p_T (toward), min bias

Σp_T density vs leading jet p_T (away), min bias

p_T distribution (transverse), leading $p_T > 5$ GeV

p_T distribution (transverse), leading $p_T > 30$ GeV

CDF Run I underlying event in MIN/MAX-cones[14] (“MIN-MAX” analysis)

$\langle p_T^{\text{max}} \rangle$ vs. E_T^{lead} , $\sqrt{s} = 1800$ GeV

$\langle p_T^{\text{min}} \rangle$ vs. E_T^{lead} , $\sqrt{s} = 1800$ GeV

$\langle p_T^{\text{diff}} \rangle$ vs. E_T^{lead} , $\sqrt{s} = 1800$ GeV

$\langle N_{\text{max}} \rangle$ vs. E_T^{lead} , $\sqrt{s} = 1800$ GeV

$\langle N_{\text{min}} \rangle$ vs. E_T^{lead} , $\sqrt{s} = 1800$ GeV

Swiss Cheese p_T^{sum} vs. E_T^{lead} (2 jets), $\sqrt{s} = 1800$ GeV

$\langle p_T^{\text{max}} \rangle$ vs. E_T^{lead} , $\sqrt{s} = 630$ GeV

$\langle p_T^{\text{min}} \rangle$ vs. E_T^{lead} , $\sqrt{s} = 630$ GeV

$\langle p_T^{\text{diff}} \rangle$ vs. E_T^{lead} , $\sqrt{s} = 630$ GeV

Swiss Cheese p_T^{sum} vs. E_T^{lead} (2 jets), $\sqrt{s} = 630$ GeV

D0 Run II dijet angular correlations[15]

Dijet azimuthal angle, $p_T^{\text{max}} \in [75, 100]$ GeV

Dijet azimuthal angle, $p_T^{\text{max}} \in [100, 130]$ GeV

Dijet azimuthal angle, $p_T^{\text{max}} \in [130, 180]$ GeV

Dijet azimuthal angle, $p_T^{\text{max}} > 180$ GeV

CDF Run II minimum bias[16]

$\langle p_T \rangle$ of charged particles vs. N_{ch} , $\sqrt{s} = 1960$ GeV

CDF Run I Z p_T [17]

$\frac{d\sigma}{dp_T^Z}$, $\sqrt{s} = 1800$ GeV
